Optics Letters

Laser intensity-dependent nonlinear-optical effects in organic whispering gallery mode cavity microstructures

Mikhail Popov,[1,*] Evgeniy Mamonov,[1] Nikolai Mitetelo,[1] Karina Zhdanova,[1] Jada Ravi,[2] Rajadurai Chandrasekar,[2] and Tatiana Murizina[1]

[1]Department of Physics, Moscow State University, Leninskie Gory, 1, 119991 Moscow, Russia
[2]Functional Molecular Nano-/Micro-Solids Laboratory, School of Chemistry, University of Hyderabad, Prof. C. R. Rao Road, Gachibowli, Hyderabad-500046, India
*Corresponding author: popov@shg.ru

Received 19 June 2020; revised 24 July 2020; accepted 24 July 2020; posted 24 July 2020 (Doc. ID 400620); published 13 August 2020

Nonlinear microresonators are very desired for a wide variety of applications. Up-conversion processes responsible for the transformation of IR laser radiation into visible are intensity-dependent and thus rather sensitive to all involved effects, which can mask each other. In this work we study the phenomena that are the most important for possible lasing in 4-(dicyanomethylene)-2-methyl-6-(4-dimethylaminostyryl)-4 H-pyran dye spherical microresonators: the two-photon absorption and photobleaching. Based on the suggested model of the threshold-like dependence of the two-photon luminescence (TPL) on pump power, we demonstrate the role of intensity-dependent photobleaching in the appearance of the TPL and find a good agreement with the experiment. This finding is important for the analysis of lasing in nonlinear dye-based resonators.

https://doi.org/10.1364/OL.400620

Miniaturization of photonic devices based on novel functional molecular materials is one of the emerging streams of nanophotonics [1–10]. Organic materials are rather in perspective here since they can provide high exciton binding energy, strong charge-transfer mediated photoluminescence (PL), high values of optical nonlinear susceptibilities, tunable band gap, ease of miniaturization, and flexible device shapes [11,12] compared to inorganic ones [5]. These key features bring about a wide range of photonic functions of organic microstructures [13–15], including light-driven single-component tunable lasing [7,16–18]. In order to increase the PL efficiency, different types of optical structures are considered, including optical whispering gallery modes (WGMs) resonators [8,19–26], that are prospectively for biological [24], chemical [27], and temperature [28] sensing, they can be used as narrow linewidth optical filters [29] and efficient nonlinear-optical (NLO) converters exploiting the strong WGMs-assisted electromagnetic field localization [30]. The WGM spectrum reveals the shape, size, and composition of the microstructure, as well as the environmental conditions. Recently, a few examples of organic photonic microstructures supporting *multiphoton* excitation of WGM, quasi-WGM, and Fabry–Perot modes (FPs) were demonstrated [5,31]. Such nonlinear structures provide the difference in wavelengths of the up-converted PL and fundamental radiation, which is rather attractive and finds applications in the area of optical communications, medical/biological imaging, and micro-lasing.

One of the efficient methods for the fabrication of WGM and FP organic microstructures is the self-assembly technique [32], which allows us to make microspheres [33], hemispheres [5], rods [5], frustums [34], toroids [35], disks [36], wires [37], etc., with their PL emission spectra covering from UV to IR regions [9,38]. As compared to inorganic materials, organic ones experience stronger photobleaching [39], while the nonlinear effects in the presence of photobleaching in organic WGM microresonators have not been studied up to now.

Among organic dyes, 4-(dicyanomethylene)-2-methyl-6-(4-dimethylaminostyryl)-4 H-pyran (DCM) is a good candidate for the two-photon pumped PL devices, as it reveals high luminescent yield of nearly 0.7 [40] and a large two-photon absorption (TPA) cross section [41]. Excitation of WGMs in DCM-based self-assembled microstructures for single- and two-photon pumped PL has been demonstrated quite recently [5,33]. Here, we study nonlinear absorption and photobleaching in spherical DCM microresonators. We show that the pump power dependence of the TPL intensity for individual WGMs reveals a threshold-like character, which is interpreted as the appearance of the nonlinear photobleaching effect.

Disordered arrays of organic DCM dye microspheres of 5–10 μm in diameter were formed by the solvent-assisted self-assembly technique; the characterization details can be found elsewhere [5,33], and the scanning electron microscope (SEM) image is shown in Fig. 1(a). For the NLO experiments, we used a two-photon microscopy set-up based on a femtosecond Ti:sapphire laser operating at an 810 nm wavelength [Fig. 1(b)], where the DCM linear absorption is negligible [33]. The TPL signal, when necessary, was analyzed by a spectrometer (with the spectral resolution of 1 nm) and collected by a photomultiplier tube (PMT, Hamamatsu R4220). The laser spot size in the

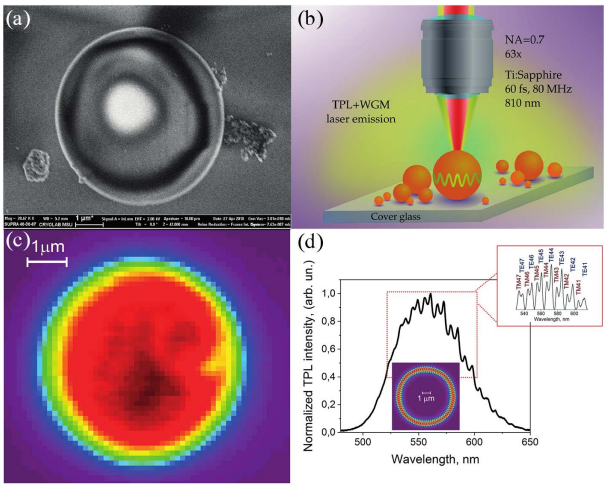

Fig. 1. (a) SEM image of a DCM microsphere, (b) schematic representation of the two-photon confocal microscopy set-up, (c) TPL distribution over a 5 μm DCM microsphere, and (d) typical TPL spectrum of a 6.5 μm microsphere excited by the 810 nm laser in the edge region. The upper inset shows the WGMs spectrum extracted from the TPL spectrum with the calculated polar mode numbers. The lower inset shows the calculated WGM energy distribution.

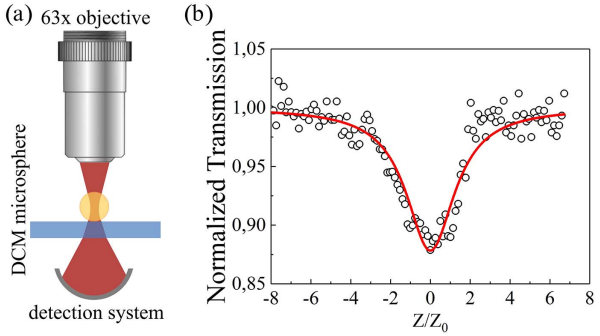

Fig. 2. (a) Scheme of the Z-scan microscopy setup. (b) Normalized transmittance $T(z/z_0)$ for a DCM microsphere of 5 μm in diameter measured by the Z-scan microscopy technique.

focus of the objective (NA = 0.7) was less than 1 μm, while the nonlinear response was detected from an area of ≈0.5 μm in diameter; so, the TPL response from the edge and center of a microsphere can be distinguished. Figure 1(c) shows TPL distribution within a single microsphere. The TPL spectrum of a microsphere of 6.5 μm in diameter with a set of peaks associated with the WGMs excitation is shown in Fig. 1(d).

Nonlinear absorption of a single microsphere was studied by the Z-scan technique [42] in transmission through a DCM particle. Nonlinear absorption is described by the nonlinear coefficient β in accordance with the definition of the total absorption $\alpha(I) = \alpha_0 + \beta I + \cdots$, where α_0 is the linear absorption coefficient, and I is the laser beam intensity. The scheme of the Z-scan microscopy technique is shown in Fig. 2(a), the relative position of the laser beam waist versus the microsphere was varied by moving the sample in the vertical z direction, and the centers of the beam waist and of the microsphere coincide at $z = 0$.

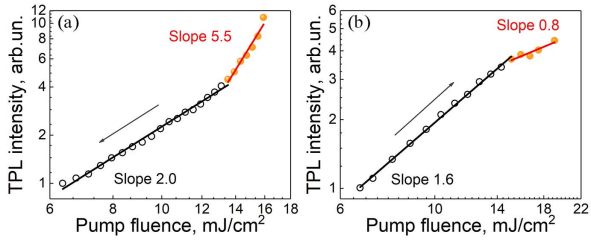

Fig. 3. Dependences of the TPL intensity on the pump fluence that is (a) decreasing and (b) increasing; the graphs are plotted in the logarithmic scales.

According to the well-known procedure, we measured the dependence of the normalized transmission $T(z)/T(\infty)$ on the relative coordinate z/z_0, where $z_0 = \frac{n\pi w_0^2}{\lambda}$ is the Rayleigh length, and w_0 is the Gaussian beam spot radius in the focal plane of the objective. Figure 2(b) shows the obtained experimental curve with a strong minimum at $z = 0$, the modulation depth being more than 10%; it corresponds to the nonlinear absorption coefficient $\beta = 4$ cm/GW, which is typical for an organic specimen [43].

Thus, even being arranged in a microparticle, the DCM dye remains a strong nonlinear absorber with high value of the imaginary part of the third-order nonlinear susceptibility in the visible spectral range. It means that we have necessarily taken it into consideration when discussing the multiphoton NLO interaction.

In order to study the mechanisms underlying the TPL in DCM microspheres, we studied the dependence of the TPL intensity of individual WGM particles on the laser beam power focused at its edge. Figure 3(a) shows such a dependence plotted in the log-log scale as the laser fluence decreased continuously from 16 mJ/cm^2, each experimental point being the result of the TPL signal averaged for 30 s. One can see that this dependence reveals a threshold-like behavior with the kink at the laser fluence of 13.3 mJ/cm^2, where the slope changes abruptly from 5.5 down to two. This kind of dependence is one of the most important and frequently used confirmations of lasing. At the same time, different processes should be considered here, including the expected strong photobleaching.

Figure 3(b) shows similar TPL intensity dependence as described above, measured while the pump fluence was increasing. One can see that it also reveals a threshold-like behavior with the critical fluence being again about 15.1 mJ/cm^2, where the slope decreases from 1.6 to 0.8.

In order to study the kinetics of the nonlinear luminescence in the DCM microspheres, we studied the time dependencies of the TPL intensity for a set of values of the laser fluence; the corresponding dependencies are shown in Fig. 4(a). For convenience, each of the curves is normalized by the TPL intensity at $t = 0$. One can see that the TPL signal decreases continuously with the exposition time; the decay rate is larger for higher values of the laser fluence. These properties are typical for the photobleaching effect that leads to irreversible TPL power dependencies. Thus, the kinetics of photobleaching should be necessarily taken into account when analyzing the TPL effect.

As the first approximation, the time dependences of the TPL intensity can be described by the exponential decay function characterized by the coefficient $\gamma(I)$ through $A(I, t) = A_0 e^{-\gamma(I)t}$. The dependence $\gamma(I)$ estimated from

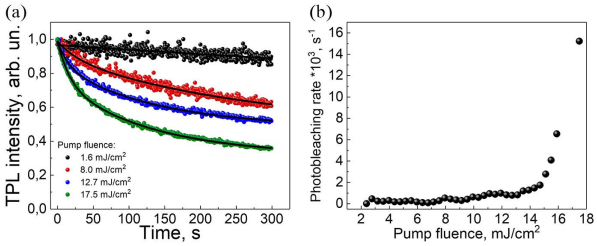

Fig. 4. Typical decay curves of PL over time with (a) bi-exponential approximation and (b) dependence of photobleaching rate constant on pump intensity.

the experimental data is shown in Fig. 4(b). It can be seen that the photobleaching rate first grows as the fluence increases to approximately 14 mJ/cm^2, afterwards a sharp rise of γ is observed.

The dependences of the TPL intensity on the pump fluence shown in Fig. 3 can be described as follows. Let us consider the nonlinear k-photon process with the intensity I^{NLO} given by the kth power of the intensity of the incident radiation, I^{pump}:

$$I^{\mathrm{NLO}}(k\omega) = A \cdot I^{\mathrm{pump}}(\omega)^k, \tag{1}$$

where ω is the frequency of the laser radiation, and A is the parameter that depends on the effective nonlinear susceptibility of the $(k+1)$th order, $\chi_{\mathrm{eff}}^{(k+1)}$, on the volume of the irradiated area, quantum efficiency of the detection system, etc. and does not depend directly on the parameters of the pump radiation. In what follows, the upper indexes will be omitted.

Let us consider different values of the pump intensity $\{I_j\}$ enumerated by the index j. The TPL intensity observed for the illumination of a medium by the laser beam with the intensity I_j and averaged over a certain collection time Δt, which corresponds to each of the experimental points shown in Fig. 3(a), can be expressed as

$$\begin{aligned}\overline{S_j} &= \frac{1}{\Delta t}\int_0^{\Delta t} I^{\mathrm{NLO}}(I_j, \tau)\mathrm{d}\tau \\ &= \frac{1}{\Delta t}\int_0^{\Delta t} A(I_j, \tau) I_j^k \mathrm{d}\tau = \overline{A(I_j)} I_j^k.\end{aligned} \tag{2}$$

In the presence of photobleaching, A is a continuously decreasing function of time; in the general case, it can be described by a multi-exponential decay [44] for a given pump intensity I_j:

$$A(I_j, t) = B_j + \sum_{l=1}^{n} A_{0,j,l} e^{-\gamma_l(I_j)t}, \tag{3}$$

where $\gamma_l(I_j)$ is the intensity-dependent decay coefficient corresponding to the photobleaching rate. The analysis shows that two terms ($n = 2$) are enough to fit the experimental dependencies [Fig. 4(a)]. It is worth noting that in this case the decay rates differ by more than an order of magnitude. Moreover, at typical timescale of the TPL spectrum capturing (30 s or less) only one term is needed to fit, so we can use the following formula:

$$A(I_j, t) = A_{0,j} e^{-\gamma(I_j)t}. \tag{4}$$

The values of γ for different I_j were estimated from the experimental curves [Fig. 4(a)]; Fig. 4(b) shows the corresponding result.

Let us discuss the dependence of the TPL response of the dye on the fluence of the laser radiation shown in Fig. 3. If we assume that $A_{0,j}$ is a constant during the measurement of each point of this dependence for the fixed intensity I_j, and $A(I_j, t)$ is described by Eq. (4) during the Δt time interval, then the parameter $A_{0,j}$ that should be used for the estimation of the $I^{\mathrm{NLO}}(I_j)$ is given by the following recurrent relation:

$$A_{0,j+1} = A(I_{j+1}, 0) = A_{0,j} e^{-\Gamma_j}, \tag{5}$$

where $\Gamma_j = \gamma(I_j)\Delta t$ and $A_0 \equiv A_{0,1}$. In this approximation, the TPL signal measured on the jth step corresponding to the pump intensity I_j is expressed by

$$\overline{S_j} = A_0 e^{-\sum_{i=1}^{j-1}\Gamma_i} \frac{(1 - e^{-\Gamma_j})}{\Gamma_j} I_j^k = \overline{A(I_j)} I_j^k. \tag{6}$$

In the double logarithmic scale, this gives for the slope

$$\ln(\overline{S_j}) = k * \ln(I_j) + \ln(\overline{A(I_j)}). \tag{7}$$

Let us denote $\ln(I_j) = x_j$ and $\ln(\overline{S_j}) = y_j$, so that Eq. (7) takes the form

$$y_j = k x_j + \ln(\overline{A(e^{x_j})}). \tag{8}$$

Then, the derivative of the TPL power dependence can be expressed as

$$\frac{\Delta y}{\Delta x} = k\left(1 + \frac{\ln(\overline{A(I_j)}/\overline{A(I_{j+1})})}{\ln(I_j^k/I_{j+1}^k)}\right), \tag{9}$$

where $\Delta x = x_j - x_{j+1}$ and $\Delta y = y_j - y_{j+1}$. Thus, the deviation of the slope of this logarithmic dependence from the expected value k is determined by the second term in the brackets, i.e., by the ratio of the two factors: the decrease of the function $A(I)$ due to photobleaching and decrease of the TPL signal caused by the change of the pump radiation.

Let us first consider the TPL power dependence measured when the pump intensity was decreasing, which corresponds to the case $I_{j+1} = I_j - \Delta I_j$, $\Delta I_j > 0$. In this approximation one gets

$$\begin{aligned}\ln(I_j/I_{j+1}) &= \ln\left(1 + \frac{\Delta I_j}{I_{j+1}}\right) \approx \frac{\Delta I_j}{I_{j+1}}, \\ \frac{\Delta y}{\Delta x} &\approx k + \frac{\Gamma_j + \Gamma_{j+1}}{2\Delta I_j / I_{j+1}}.\end{aligned} \tag{10}$$

In the opposite case of increasing pump intensity, when $\Delta I_j = -|\Delta I_j|$, one gets

$$\frac{\Delta y}{\Delta x} \approx k - \frac{\Gamma_j + \Gamma_{j+1}}{2\,|\Delta I_j|/I_{j+1}}. \tag{11}$$

Thus, if the step in the pump intensity $|\Delta I_j|$ is small enough, and the exposition time is large (so does Γ_j), the deviation of the slope coefficient from k can be arbitrarily large.

Figure 5 shows the dependences of the TPL intensity on the pump fluence calculated using Eq. (6) when taking typical $|\Delta I_j|$

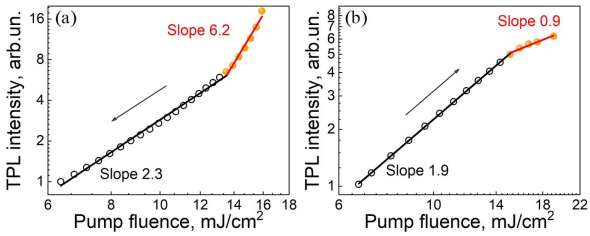

Fig. 5. Calculated dependencies of the TPL intensity on the pump fluence that is (a) decreasing and (b) increasing.

and Δt values used in the experiment; one can see a qualitative agreement of theoretical and experimental data. These dependences look like they have a kink at a certain value of the laser fluence, where the slope of the curve changes in different ways when the pump fluence is increasing or decreasing. The increase of the slope for the decreasing laser fluence can be confused with the sign of lasing. Meanwhile, the nature of this kink has nothing in common with lasing and is due to the intensity-dependent photobleaching.

Summing up, we studied the dependence of the NLO response on the intensity of the exciting radiation. Using the modified Z-scan technique, the TPA coefficient of a single DCM microsphere of 4 GW/cm was estimated. The power dependence of the TPL intensity of a single WGM showed a threshold-like dependence treated usually as an intrinsic property of lasing. In accordance with the proposed simple theoretical model, we explain this dependence as the result of photobleaching of the DCM dye. These results demonstrate the principal role of photobleaching in the power dependencies of the PL, which should be necessarily taken into account when analyzing the lasing in organic microstructures.

Funding. Russian Foundation for Basic Research (18-32-20178, 19-32-90265); Department of Science and Technology, Ministry of Science and Technology, India (INT/RUS/RSF/P-05); Foundation for the Advancement of Theoretical Physics and Mathematics (19-2-6-186-1); Foundation for the Advancement of Theoretical Physics and Mathematics (17-21-2152-1).

Disclosures. The authors declare no conflicts of interest.

REFERENCES

1. P. Peumans, A. Yakimov, and S. R. Forrest, J. Appl. Phys. **93**, 3693 (2003).
2. H. Hoppe and N. S. Sariciftci, J. Mater. Res. **19**, 1924 (2004).
3. J. Anthony, Angew. Chem. (Int. Ed.) **47**, 452 (2008).
4. H. E. Katz and J. Huang, Annu. Rev. Mater. Res. **39**, 71 (2009).
5. D. Venkatakrishnarao and R. Chandrasekar, Adv. Opt. Mater. **4**, 112 (2016).
6. L. Hung and C. Chen, Mater. Sci. Eng. R **39**, 143 (2002).
7. W. Zhang, J. Yao, and Y. S. Zhao, Acc. Chem. Res. **49**, 1691 (2016).
8. D. Venkatakrishnarao, E. A. Mamonov, T. V. Murzina, and R. Chandrasekar, Adv. Opt. Mater. **6**, 1800343 (2018).
9. R. Chandrasekar, Phys. Chem. Chem. Phys. **16**, 7173 (2014).
10. N. Chandrasekhar, S. Basak, M. A. Mohiddon, and R. Chandrasekar, ACS Appl. Mater. Interfaces **6**, 1488 (2014).
11. M. Annadhasan, D. P. Karothu, R. Chinnasamy, L. Catalano, E. Ahmed, S. Ghosh, P. Naumov, and R. Chandrasekar, Angew. Chem. (Int. Ed.) **59**, 13821 (2020).
12. M. Annadhasan, A. R. Agrawal, S. Bhunia, V. V. Pradeep, S. S. Zade, C. M. Reddy, and R. Chandrasekar, Angew. Chem. (Int. Ed.) **59**, 13852 (2020).
13. J. Clark and G. Lanzani, Nat. Photonics **4**, 438 (2010).
14. J. Zhao, Y. Yan, Z. Gao, Y. Du, H. Dong, J. Yao, and Y. S. Zhao, Nat. Commun. **10**, 870 (2019).
15. C. Zhang, C.-L. Zou, Y. Zhao, C.-H. Dong, C. Wei, H. Wang, Y. Liu, G.-C. Guo, J. Yao, and Y. S. Zhao, Sci. Adv. **1**, e1500257 (2015).
16. X. Wang, Q. Liao, H. Li, S. Bai, Y. Wu, X. Lu, H. Hu, Q. Shi, and H. Fu, J. Am. Chem. Soc. **137**, 9289 (2015).
17. H. Dong, C. Zhang, X. Lin, Z. Zhou, J. Yao, and Y. S. Zhao, Nano Lett. **17**, 91 (2017).
18. R. Vattikunta, D. Venkatakrishnarao, C. Sahoo, S. R. G. Naraharisetty, D. Narayana Rao, K. Müllen, and R. Chandrasekar, ACS Appl. Mater. Interfaces **10**, 16723 (2018).
19. S. Kushida, D. Okada, F. Sasaki, Z.-H. Lin, J.-S. Huang, and Y. Yamamoto, Adv. Opt. Mater. **5**, 1700123 (2017).
20. D. Okada, T. Nakamura, D. Braam, T. D. Dao, S. Ishii, T. Nagao, A. Lorke, T. Nabeshima, and Y. Yamamoto, ACS Nano **10**, 7058 (2016).
21. V. D. Ta, R. Chen, and H. D. Sun, Sci. Rep. **3**, 1362 (2013).
22. Y. C. Tao, X. D. Wang, and L. S. Liao, J. Mater. Chem. C **7**, 3443 (2019).
23. R. Chikkaraddy, A. Dasgupta, S. D. Gupta, and G. V. P. Kumar, Appl. Phys. Lett. **103**, 031112 (2013).
24. F. Vollmer and S. Arnold, Nat. Methods **5**, 591 (2008).
25. M. R. Foreman, J. D. Swaim, and F. Vollmer, Adv. Opt. Photon. **7**, 168 (2015).
26. D. V. Strekalov, C. Marquardt, A. B. Matsko, H. G. L. Schwefel, and G. Leuchs, J. Opt. **18**, 123002 (2016).
27. L. He, Ş. K. Özdemir, and L. Yang, Laser Photon. Rev. **7**, 60 (2013).
28. G. Guan, S. Arnold, and M. V. Otugen, AIAA J. **44**, 2385 (2006).
29. J. P. Rezac and A. T. Rosenberger, Opt. Express **8**, 605 (2001).
30. D. Venkatakrishnarao, C. Sahoo, E. A. Mamonov, V. B. Novikov, N. V. Mitetelo, S. R. G. Naraharisetty, T. V. Murzina, and R. Chandrasekar, J. Mater. Chem. C **5**, 12349 (2017).
31. Y. Xu, Q. Chen, C. Zhang, R. Wang, H. Wu, X. Zhang, G. Xing, W. W. Yu, X. Wang, Y. Zhang, and M. Xiao, J. Am. Chem. Soc. **138**, 3761 (2016).
32. C. Wei, S.-Y. Liu, C.-L. Zou, Y. Liu, J. Yao, and Y. S. Zhao, J. Am. Chem. Soc. **137**, 62 (2015).
33. E. A. Mamonov, A. I. Maydykovskiy, N. V. Mitetelo, D. Venkatakrishnarao, R. Chandrasekar, and T. V. Murzina, Laser Phys. Lett. **15**, 035401 (2018).
34. D. Venkatakrishnarao, Y. S. L. V. Narayana, M. A. Mohaiddon, E. A. Mamonov, N. Mitetelo, I. A. Kolmychek, A. I. Maydykovskiy, V. B. Novikov, T. V. Murzina, and R. Chandrasekar, Adv. Mater. **29**, 1605260 (2017).
35. E. Lee, Y.-H. Jeong, J.-K. Kim, and M. Lee, Macromolecules **40**, 8355 (2007).
36. Q. Liao, K. Hu, H. Zhang, X. Wang, J. Yao, and H. Fu, Adv. Mater. **27**, 3405 (2015).
37. D. H. Kim, J. T. Han, Y. D. Park, Y. Jang, J. H. Cho, M. Hwang, and K. Cho, Adv. Mater. **18**, 719 (2006).
38. G. M. Whitesides and B. Grzybowski, Science **295**, 2418 (2002).
39. G. Oster and N. Wotherspoon, J. Chem. Phys. **22**, 157 (1954).
40. P. Hammond, Opt. Commun. **29**, 331 (1979).
41. A. V. Kulinich and A. A. Ishchenko, Russ. Chem. Rev. **78**, 141 (2009).
42. E. W. V. Stryland and M. Sheik-Bahae, Proc. SPIE **10291**, 488 (1997).
43. G. S. He, L.-S. Tan, Q. Zheng, and P. N. Prasad, Chem. Rev. **108**, 1245 (2008).
44. A. J. Berglund, J. Chem. Phys. **121**, 2899 (2004).